*Sensors and Materials*, Vol. 38, No. 7 (2026) 4207–4218
MYU Tokyo


S & M 4559

# Spatiotemporal Analysis of Sea Level Variability along the Coast of Korea Using Long-term Observational Data

Gyu-Seok Han,[1] Seung-Bae Choi,[1] Jae-Seon Yoon,[2]
Woo-chul Kang,[3] and Hyung-Suk Kim[1*]

[1]Department of Civil Engineering, Kunsan National University,
Gunsan, Jeollabuk-do 54150, Republic of Korea
[2]Rural Research Institute, Korea Rural Community Corporation, Ansan 15634, Republic of Korea
[3]Department of Smart Infrastructure Engineering, Kongju National University,
Cheonan, Chungcheongnam-do 31080, Republic of Korea

(Received November 21, 2025; accepted July 27, 2026)

***Keywords:*** tide, mean sea level, low-pass filter, temporal and spatial changes, Lanczos filtering

Global sea level change patterns represent an average of gradual temporal changes occurring across wide areas. However, localized sea level change patterns can differ significantly. In the Republic of Korea, for instance, sea level rise along its coasts notably exceeds the global average. The specific patterns of mean sea level (MSL) change vary considerably by sea area (e.g., east, west, south, and Jeju) owing to regional differences in influencing factors. This is evident in the diverse rates of sea level rise; the west sea records the lowest at 1.36 mm/year, whereas the Jeju sea area has the highest at 5.81 mm/year, a difference of approximately 4.3 times. Crucially, the recent acceleration in sea level rise, when combined with these regional variations, where temporal and spatial changes converge, can intensify the rise, potentially creating areas highly vulnerable to sea level rise. In this study, we analyze sea level changes along the coast of South Korea using long-term tidal observation data collected at one-hour intervals from coastal tide gauge sensors. These sensors continuously measure the sea surface at a high temporal resolution (hourly), providing essential data for monitoring changes in the marine environment. Unlike past research in which MSL rise (or fall) was estimated by simply taking the arithmetic mean of observation data, our approach facilitated a sea level change analysis that simultaneously considered both temporal and spatial variations using tidal data that accounted for only long-period components. A prominent finding of the analysis is that the amount of sea level rise on the west coast of South Korea increases from the north (Yeongjong Bridge) to the south (Mokpo). The fact that sea level rise due to the long-period components (with short-period components excluded) is greater in the south (Mokpo) suggests that, from a long-term perspective, the change in MSL could be more significant in the southern region of the west coast than in the northern part.

## 1. Introduction

Sea level rise refers to the phenomenon of rising global sea levels caused by climate change. Owing to the use of fossil fuels and greenhouse gas emissions from human activities, the global

*Corresponding author: e-mail: hskim0824@kunsan.ac.kr
https://doi.org/10.18494/SAM6183

ISSN 0914-4935 
https://myukk.org/

average surface temperature has increased by approximately 1.1 °C during 2011–2020 compared with 1850–1900. As a result of global warming, the oceans have absorbed more heat than before. When seawater temperature increases, the volume of water expands, leading to a rise in sea level. Moreover, as air temperature continues to rise, ice sheets and glaciers on land melt more rapidly, and the meltwater flows into the oceans, further accelerating sea level rise.[1–3] The rise in sea level not only causes direct damage such as the flooding of low-lying coastal areas, changes in tides and waves, and alterations in sediment transport, but also interacts with storm surges and floods to create complex problems. These include impacts on the stability and functionality of coastal structures and infrastructure.[4–8]

According to the Sixth Assessment Report published in 2023 by the Intergovernmental Panel on Climate Change (IPCC),[9] the global mean sea level (MSL) rose at an average rate of 1.3 mm/year from 1901 to 1971, and this rate increased to 3.7 mm/year between 2006 and 2018. Overall, the global MSL increased by approximately 200 mm between 1901 and 2018, and the rate of increase continues to accelerate over time. In the case of South Korea, the rate of sea level rise tends to be higher than the global average. From 1989 to 2018, while the global average sea level rose at a rate of 1.8 mm per year, the waters surrounding the Korean Peninsula rose by 2.74 mm/year, and particularly around Jeju Island, the rate reached 4.75 mm/year.[10]

In reality, the intensity of factors affecting sea level changes varies across different coastal regions of Korea including the east, west, and south seas and Jeju Island, resulting in significant differences in the patterns of MSL change. The rate of sea level rise shows considerable regional variation, with the west sea recording the lowest rate at 1.36 mm/year and the Jeju coastal area exhibiting the highest at 5.81 mm/year, a difference of approximately 4.3 times.[7,11] Recent reports by the IPCC indicate that this rate of rise is highly likely to accelerate further in the future compared with the past. When the accelerating sea level rise trend and the changes in the regional rise rate are superimposed—that is, when the temporal and spatial variations of sea level are superimposed—the sea level rise shows further acceleration, potentially leading to the emergence of areas that exhibit vulnerability to sea level rise.[12]

Sea level observations in Korea are conducted in real time at tidal observation stations operated by the Korea Hydrographic and Oceanographic Agency (KHOA), using tide gauge sensors installed along the coast. These sensors continuously measure sea level with high accuracy, playing a crucial role in monitoring the marine environment and providing essential data for understanding long-term climate change and coastal ocean processes. In recent years, advancements in sensing technologies and data acquisition systems have significantly improved the accuracy, continuity, and spatial coverage of sea level observations.

In this study, the sea level changes along the Korean coastal regions were analyzed using tide gauge data. Unlike previous studies[7,11,13] in which the rise or fall of MSL was estimated by simply calculating the arithmetic average of tide gauge data, in this research, we applied the Lanczos filtering technique, one of the filtering methods based on the Fourier transform. By using tide gauge data filtered to retain only long-period components, in this study, we analyzed sea level variations while simultaneously considering both temporal and spatial changes.

## 2. Analysis Data and Methodology

In this section, we briefly review the current status of tide gauge and tidal observation data in South Korea's coastal waters for the analysis of temporal and spatial sea level variations, as well as the methods used for this analysis. On the basis of the analysis methods presented in the report, we briefly examine the limitations of conventional sea level change research and the analysis method using Lanczos filtering, which is a technique that applies the Fourier transform to overcome these limitations.

### 2.1 Collection of tidal observation data

Studies on sea level change in the Republic of Korea have primarily been conducted on the basis of tidal observation data along the coast.(14) For this study, hourly tidal observation data from all tidal observation stations operated by the KHOA were collected to analyze the spatiotemporal variations of sea level in the coastal areas. A total of 47 tidal observation stations are currently in operation. Although the observation start dates for each station vary, all observation data, including missing values, from the respective start date up to December 2021, were collected and used for the analysis.

The tidal observation stations are distributed across seven locations on the east coast, 21 on the west coast, 14 on the south coast, and four in the Jeju area. Among these, the Busan and Mokpo stations possess the longest records, with observations starting in 1956, holding approximately 65 years of tidal observation data. In contrast, the Pohang station, which began observations in September 2018, has the shortest duration of recorded data. The location of each tidal observation station by sea area, along with the duration of observation data held by each station, is shown in Fig. 1.

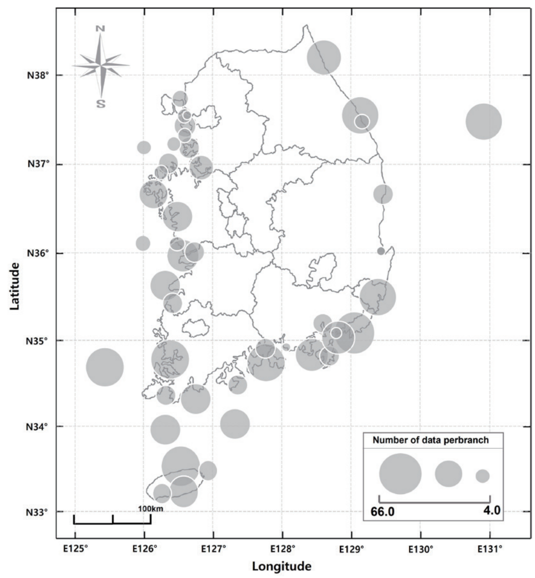


Fig. 1. Location of tidal stations and data retention period.

### 2.2 Equations

Previous studies on sea level variation have included analyses of MSL changes, estimation of extreme tidal variation rates, and investigations of long-term components.(15) The methods predominantly employed in Korean sea level change studies are to first calculate the MSL by arithmetically averaging the observed tidal data, and then to utilize it to identify the long-term trend (rise or fall) of the sea level, or to determine the highest high water level (HHWL) from the tidal data to ascertain its pattern of variation. While these approaches offer simplicity for the basic estimation of sea level variability using observed tidal data, they possess inherent difficulties in accurately projecting future sea level changes.(14,16) This limitation stems from the fact that the tidal observation data measured in coastal areas reflect the combined effects of astronomical tides, meteorological tides, and climate change, and the analysis is conducted without effectively distinguishing between these separate components.

In this study, a low-pass filter was used to exclude short-period components such as astronomical and meteorological tides. By focusing on the long-term components, only the factors that affect long-term sea level variations are considered in the analysis. The cutoff frequency for the low-pass filter was set at 0.889 cycles/day (27 h) to filter out the four major tidal constituents dominant in Korean waters, particularly components in the diurnal range and at higher frequencies. The $Q_1$ tide, with a period of 26.87 h, was chosen as the reference because it is the longest-period diurnal constituent, despite having less impact than the four major constituents. The filter allows long-period components to be included while eliminating short-period ones. Note that the sharp drop to zero in the frequency response at the cutoff point may cause Gibbs oscillations owing to the resulting discontinuity. To achieve this, the Lanczos filtering method based on the Fourier transform(15,17,18) was applied. This filtering technique is widely used in the analysis of oceanographic observational data, as it can significantly reduce the amplitude of Gibbs oscillations that commonly occur when applying low-pass filters.(17,19) The transformation of the time series using Lanczos filtering is performed using

$$Y_n = \sum_{k=-M}^{M} W_k x_{n-k} \cdot \left(n = 0,\ 1,\ \ldots,\ N-1\right) \tag{1}$$

Here, $y_n$ is the transformed output data, $w_k$ is the weight, and $x_{n-k}$ is the input data, which consists of $N$ data points ($x_0$, $x_1$, ..., $x_{n-1}$). $M$ is an arbitrary integer. Taking the Fourier transform of $y_n$ in Eq. (1) yields

$$Y\left(\omega\right) = \sum_{n=-M}^{M} Y_n e^{-i\omega n\Delta t} = \sum_{n=-M}^{M} \omega_k e^{-i\omega k\Delta t} \sum_{n=-M}^{M} x_{n-k} e^{-i\omega(n-k)\Delta t} = W\left(\omega\right) X\left(\omega\right). \tag{2}$$

Here, $W(\omega)$ is the frequency response function that determines the transformation from the input value to the output value, and $\omega = 2\pi f$ is the cut-off frequency. The weight $w_k$ presented in Eq. (1) and the response function $W(\omega)$ in Eq. (2) are determined by

$$W(\omega) = \frac{Y(\omega)}{X(\omega)} = \sum_{n=-M}^{M} \omega_k e^{-i\omega k \Delta t} = \omega_o + \sum_{n=-M}^{M} \omega_k \cos\frac{\pi k \omega}{\omega_N}, \tag{3}$$

$$\omega_k = \frac{1}{\omega_N} \int_0^{\omega_N} H(\omega) \cos\left(\frac{\pi k \omega}{\omega_N}\right) d_\omega, \tag{4}$$

where $\Delta t$ represents the data time interval, which is 1 h, and $w_N$ is the Nyquist frequency, which has a value of 1/2 the period of the data interval. In the case of a low-pass filter, once the cut-off frequency $w_c$ is set, the weights ($w_k$) in the interval $0 \leq |\omega| \leq \omega_c$ are given by

$$\omega_k = \frac{\omega_c}{\omega_N}\left[\left(\sin\frac{\pi k \omega}{\omega_N}\right) \Big/ \frac{\pi k \omega}{\omega_N}\right]. \tag{5}$$

Further details on Lanczos filtering have been given by Claude[18] and Richard and William.[20]

## 3. Results and Discussion

In this section, on the basis of the analysis method presented in Sect. 2, we analyzed the monthly MSL using the results of Lanczos filtering for all tide gauge observation stations in the Korean coastal zone, and simultaneously examined the spatiotemporal variation pattern of sea level using a Hovmöller diagram.

### 3.1 MSL analysis

Among the various methods used to study sea level variation, the most representative approach is to calculate the MSL and analyze its changes.[7] The monitoring of MSL is the simplest way to intuitively grasp sea level variation patterns, which is why most past studies have presented monthly (or annual) MSL values. The raw tidal data observed at each tidal station include the effects of all tidal constituents; however, for accurate analysis, short-term variability should be excluded and the long-term components should be considered.[14,21] Accordingly, monthly MSL analysis utilizing the results of Lanczos filtering[15] was performed for all tide gauge observation stations.

The MSL values calculated using the Lanczos filtering results obtained in this study were compared with the MSL values provided by the KHOA for validation. The results of this comparison are shown in Fig. 2.

To quantitatively assess the degree of agreement between these results, the relative accuracy ($RA$) was calculated using Eq. (6) and is expressed as the percentage of the Lanczos-filtered monthly MSL values relative to the MSL values provided by the KHOA. Since $RA$ is around

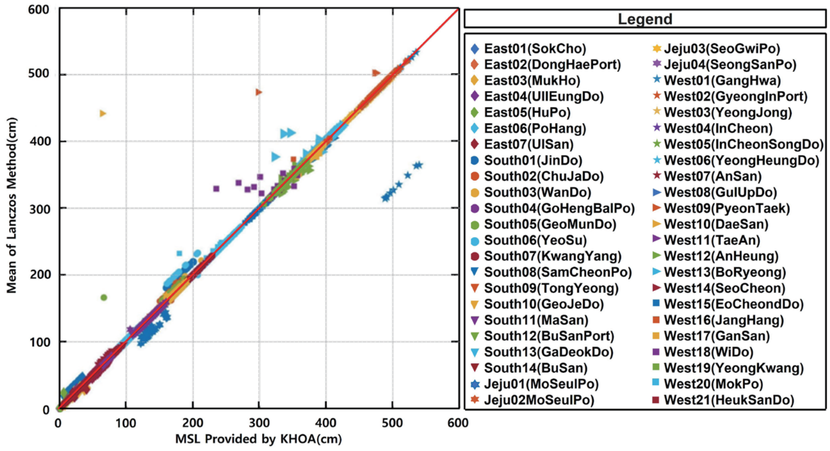


Fig. 2. (Color online) Results of comparison of monthly MSL values at all points.

100% at all stations, it can be concluded that the calculated monthly MSL values in this study are generally within the valid range.

$$RA = \frac{Mean\ of\ Lanczos\ Method}{MSL\left(by\ KHOA\right)} \times 100 \tag{6}$$

### 3.2 Tidal analysis considering long-period components

In this study, analysis was performed using tidal observation data provided by the KHOA. Initially, a preprocessing stage was conducted to remove erroneous values contained in the observation data, specifically by eliminating continuously recorded values of ‘0’ or values that were entirely irrelevant to the tidal fluctuation trend. Following data preprocessing, a low-pass filter was applied to remove short-period variability components, such as astronomical and meteorological tides. Among the results derived from this process, the data from the Gunsan tidal station on the west coast are presented as a representative example in Fig. 3.

Figure 3(a) presents the raw tidal observation data recorded at the station, whereas Fig. 3(b) shows the result of low-pass filtering, where only long-period components were considered and short-period components were excluded. The filtering result demonstrates a significant reduction in the tidal range compared with the raw data, as both the diurnal tides and semidiurnal tides, which account for the majority of the tidal components, were removed.

An examination of the frequency–amplitude spectra before and after filtering, presented together in Figs. 3(c) and 3(d), shows that in Fig. 3(c), the frequency with the highest amplitude is approximately 2 cycles/day, followed by a secondary peak at about 1 cycle/day. These correspond to the semidiurnal tide, which occurs twice a day, and the diurnal tide, which occurs once a day. Such results can be attributed to the effect of the four principal tidal constituents that predominantly affect the tidal characteristics in Korean coastal waters. Furthermore, in Fig. 3(d), which shows the spectrum after applying the low-pass filter, it can be confirmed that these frequencies have been effectively removed.

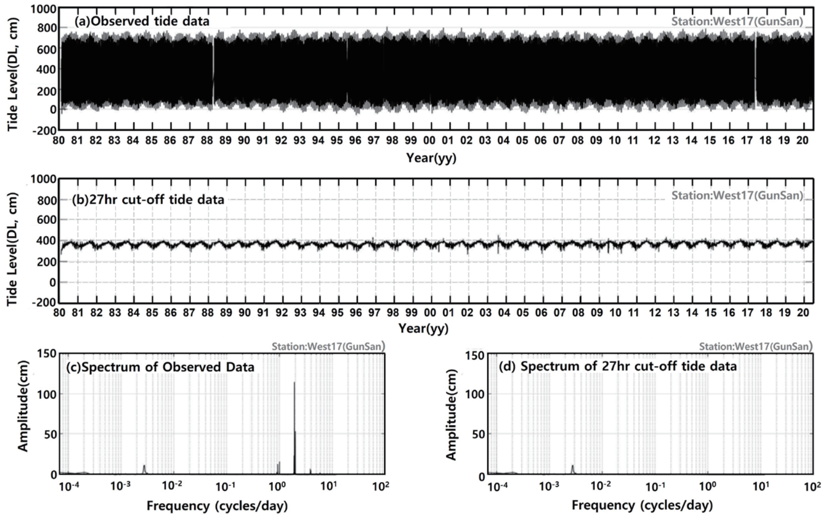


Fig. 3. Results of the tide analysis using the low-pass filter of Lanczos filtering (Gunsan on the west coast).

This characteristic is particularly prominent on the west and south coasts, where the effect of tides is dominant, whereas the east coast exhibits a different pattern. The results for the Sokcho tide gauge station, which represents the east coast, are shown in Fig. 4. The observed tidal range at this site is much smaller than that along the west coast, and the amplitudes corresponding to the semidiurnal and diurnal tidal frequencies are barely noticeable. This indicates that, along the east coast, the effect of astronomical tides with frequencies equal to or lower than the diurnal tide is highly limited.

### 3.3 Temporal variation patterns of sea level

The variation in sea level is not uniform over time; its rate of change can either accelerate or decelerate. In this study, two methods were used to perform data splicing (or data joining) to examine the temporal variation patterns in each sea area. First, to identify changes in the monthly MSL, nonlinear splicing was performed using a multidimensional smoothing spline. The multidimensional smoothing spline, denoted as *S*, generates the spline that minimizes the following Eq. (7).

$$P\sum_{i}\left(Y_i - S(x_i)\right)^2 + \left(1-P\right)\int\left(\frac{d^2s}{dx^2}\right)^2 dx \tag{7}$$

Here, $x_i$ and $y_i$ represent the input data corresponding to time and tide level, respectively, and $P$ is the smoothing parameter, which takes a value between 0 and 1. The fitting was performed so that Eq. (7) can be automatically minimized. The results of the smoothing spline fit using Eq. (7) are exemplified by the Wando tide gauge station on the south coast, as shown in Fig. 5.

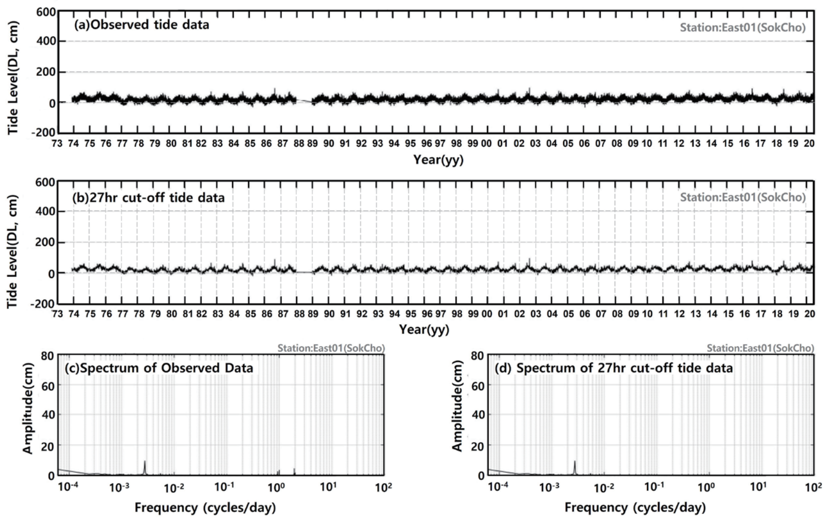


Fig. 4. Results of tide analysis using the low-pass filter of Lanczos filtering (Sokcho on the east coast).

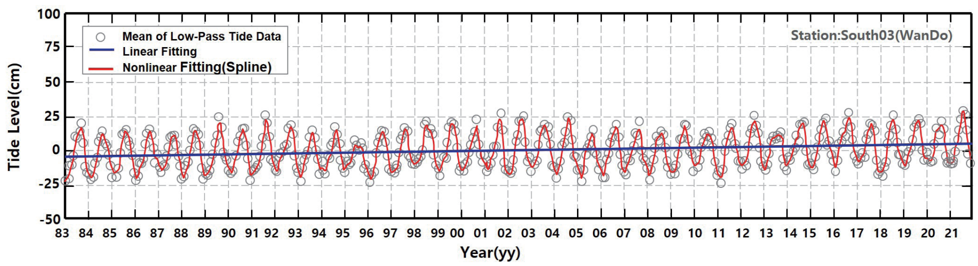


Fig. 5. (Color online) Linear and nonlinear fitting of low-pass filtering data (Wando on the south coast).

The results of the smoothing spline splicing curve derived using Eq. (6) are presented alongside the analysis of the sea level variation pattern using linear fitting in this study, as shown in Fig. 5. This linear fitting was performed to quantitatively calculate and present the trend of sea level rise (or fall), consistent with approaches in previous studies on sea level change analysis.

The analysis of the temporal variation pattern of the sea level was performed for all tidal stations using the splicing curves derived by the two methods. The results for the east and west coasts showed a similar pattern to the analysis results of the Wando tidal station on the south coast (see Fig. 6). Specifically, the sea level exhibits repeated cycles of rising and falling in accordance with the seasons, and while there are differences in the quantitative amount of rise (or fall), the temporal variation pattern of the sea level was found to be generally similar.

### 3.4 Spatiotemporal variations of sea level

As previously mentioned, sea level rise can be accelerated when the temporal variation patterns of the sea level and the rise rates of the regional location in each sea area overlap.[12] In

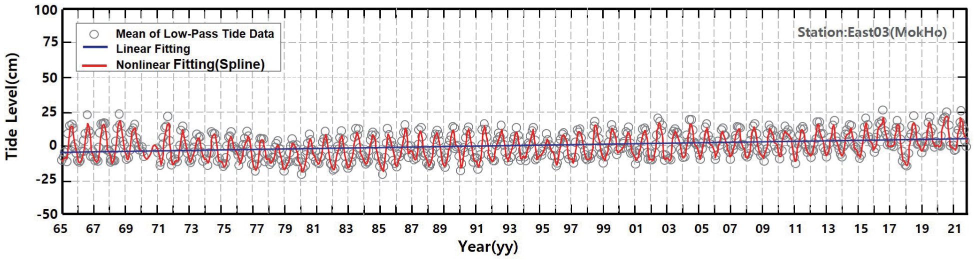


Fig. 6. (Color online) Linear and nonlinear fittings of low-pass filtering data (Mukho on the east coast).

the case of South Korea, the tides of the east, west, and south coasts exhibit distinct characteristics, necessitating the analysis of sea level variation patterns for each sea area individually. Considering this, it is crucial to identify areas vulnerable to sea level rise.

In this study, the Hovmöller diagram[22] was employed to analyze the spatiotemporal changes in sea levels and to clearly identify their spatial distribution and movement patterns. By plotting time on the *X*-axis and latitude (or longitude) on the *Y*-axis, these diagrams provide an effective visualization of how key variables change simultaneously over time and space, making it easier to track their distribution and movement trends.

Therefore, the Hovmöller diagram serves as a basis for comprehensively understanding the temporal and spatial traits of tides by visualizing water level changes along the time–latitude direction. Specifically, the periodic fluctuations in sea level deviations and the latitude-dependent differences in phase and amplitude represent the distinct marine dynamical properties inherent to the coastal waters of the east, west, and south seas of Korea. Meanwhile, using the temporal sea level change data for each tide station presented above, we constructed the Hovmöller diagram for each sea area regarding sea level changes along the east, west, and south coasts of South Korea, and the patterns of sea level change were analyzed.

A look at the representative results for the west coast (see Fig. 7), for which there are long-term observation data and a relatively high number of tidal stations that allow for a more detailed examination of the sea level's temporal and spatial variations, reveals that the magnitude of sea level rise increases as one moves from the northern part of the west coast (Yeongjong Bridge) toward the southern part (Mokpo). The region and period corresponding to the lower right-hand side of Fig. 7 (near Mokpo, after the 2000s) are distinctly marked in red. This indicates that the sea level height in this area is more than 20 cm higher than the average sea level for that sea region, and this elevated state is maintained for a longer duration.

Generally, the tidal range tends to increase from the southern to the northern part of the west coast. However, since astronomical tides with periods shorter than one day were removed through low-pass filtering, the results shown here reflect only the long-period components. The fact that sea level rise driven by long-period components is greater in the southern region (Mokpo) suggests that, from a long-term perspective, variations in MSL are likely to be more pronounced in the southern part of the west coast than in the northern part (Yeongjong Bridge). Therefore, the southern region can be interpreted as being more vulnerable to sea level rise.

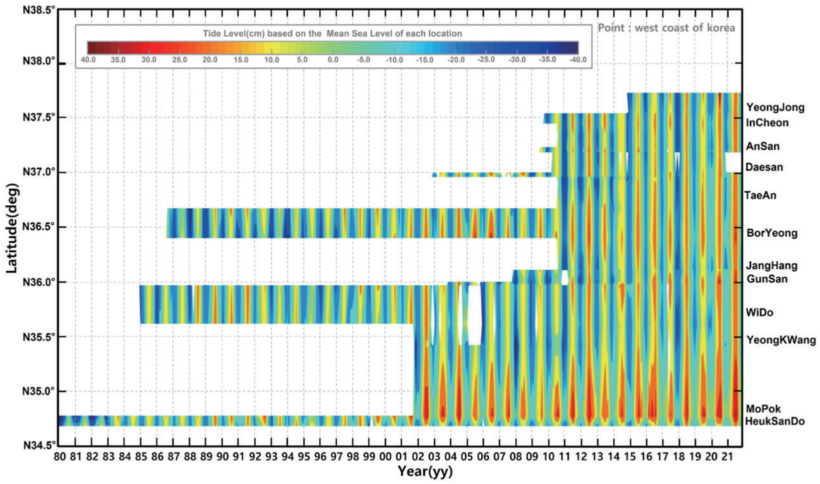


Fig. 7. (Color online) Temporal and spatial changes of sea level along the west coast.

## 4. Conclusions and Significance

This study was conducted to comprehensively analyze the temporal and spatial variation patterns of the sea level using tide gauge data observed along the domestic coast of South Korea. Fourier-based Lanczos filtering was applied to exclude short-period variability components (under 27 h), such as astronomical and meteorological tides, focusing the analysis solely on long-period factors that induce sea level changes.

The application of Lanczos filtering(14) confirmed that dominant tidal components, such as diurnal and semidiurnal tides, were effectively removed, resulting in a significantly reduced sea level compared with the raw data. However, despite the filtering of short-period components, a variability pattern with an approximately one-year period persisted, which was confirmed to be due to the effect of other long-period astronomical tides.

Analysis of the long-term sea level change pattern using the calculated monthly MSL data showed that linear fitting confirmed a general upward trend in sea level at the majority of observation stations, allowing for the quantitative determination of the long-term trend. Simultaneously, the results of nonlinear analysis via multidimensional smoothing spline splicing demonstrated a distinct seasonal variation, evidenced by the repetitive pattern of sea level rise in the summer and fall in the winter each year.

Furthermore, Hovmöller diagrams(22) were constructed using the temporal variation data of the sea level for each tidal station to simultaneously identify the temporal and spatial characteristics of sea level change. The analysis confirmed that in all sea areas, the magnitude of sea level change was greater and higher in recent years than in the past. Specifically, on the west coast, where long-term observation data are abundant, a significant spatial asymmetry was observed, with the magnitude of sea level rise being considerably greater in the southern region (Mokpo) than in the northern region (Yeongjong Bridge). This implies that the southern west coast region sustains a higher sea level than the regional mean for a relatively longer duration, suggesting that this area may be a vulnerable zone owing to sea level rise.

In conclusion, the integrated analysis method utilizing Lanczos filtering and the Hovmöller diagram applied in this study is highly significant, as it facilitates a precise analysis that considers only long-period components while simultaneously capturing the spatiotemporal variation patterns of the sea level. This analytical technique is capable of rapidly and accurately processing large amounts of observation data and can be effectively applied regardless of differences in the quality of observation records across stations, thus serving as crucial foundational data for long-term sea level variability analysis in domestic coastal waters.

## Acknowledgments

This work is financially supported by Korea Ministry of Climate, Energy, Environment (MCEE) under the Climate Resilient R&D Project for Water-Related Disaster Management (RS-2024-00397821).

## References

1 S. C. Cha and J. H. Moon: Ocean Polar Res. **41** (2019) 121.
2 S. M. Oh, S. J. Kwon, J. I. Moon, and E. I. Lee: J. Korean Soc. Coastal Ocean Eng. **23** (2011) 236.
3 W. H. Kim: UNCLOS 40th Anniversary Academic Conf. UN Convention on the Law of the Sea and the Transformation of the Maritime Order (2022).
4 Korea Hydrographic and Oceanographic Administration (KHOA): A study on the sea level change by global warming (II) (Ministry of land, infrastucture and transport, 2010).
5 R. J. Nicholls: Phys. Chem. Earth **27** (2002) 1455.
6 T. Wahl, S. Jain, J. Bender, S. D. Meyers, and M. E. Luther: Nat. Clim. Change **5** (2015) 1093.
7 J. J. Yoon and S.I. Kim: J. Korean Society of Hazard Mitigation **12** (2012) 299.
8 D. T. Pugh: Tides, Surges and Mean Sea-Level: A Handbook for Engineers and Scientists (John Wiley & Sons Ltd., 1987) 486.
9 IPCC. Climate Change 2023: Synthesis Report. Contribution of Working Groups I, II and III to the Sixth Assessment Report of the Intergovernmental Panel on Climate Change, Core Writing Team, H. Lee and J. Romero Eds. (Geneva, Switzerland, 2023) 184. https://doi.org/10.59327/IPCC/AR6-9789291691647
10 S. M. Oh, S. H. Kim, M. Y. Kim, and K. S. Kim: (National R&D Research Report) A Study on Predicting Sea Level Change Due to Global Warming (Cheju National University, 2011).
11 Korea Hydrographic and Oceanographic Administration (KHOA): Detailed Analysis and Prediction (3rd) of Sea level Change in Korea (2011).
12 A. Valle-Levinson, A. Dutton, and J. B. Martin: Geophys Res. **44** (2017) 7876. https://doi.org/10.1002/2017GL073926
13 J. W. Kang, S. R. Moon, and N. S. Oh: J. Korean Soc. Coastal Ocean Eng. **25** (2005) 255.
14 T. S. Jung: J. Korean Soc. Coastal Ocean Eng. **26** (2014) 120.
15 C. Lanczos: Applied Analysis Prentice-Hall (1956) 539.
16 T. S. Jung: J. Korean Soc. Coastal Ocean Eng. **26** (2014) 120.
17 J. W. Kang, S. J. Park, and M. W. Park: J. Korean Soc. Coastal Ocean Eng. **20** (2008) 14.
18 E. D. Claude: J. Appl. Meteorol. **18** (1979) 1016.
19 A. W. Roy and H. Cynthia: J. Phys. Oceanogr. **12** (1981) 112.
20 E. T. Richard and J. E. William: Data Analysis Methods in Physical Oceanography, (Elsevier, 2014) 3rd ed.
21 J. Jensen, T. Wahl, and T. Frank: Improved Estimates on Mean Sea Level Change in the South-eastern North Sea since 1843, J. M. Smith and P. Lynett Eds., Proc. 32nd Conf. Coastal Engineering (in CD) (Shanghai, China, 2010) 10.
22 E. Hovmöller: Tellus **1** (1949) 62. https://doi.org/10.1111/j.2153-3490.1949.tb01260

## About the Authors


**Gyu-Seok Han** is currently pursuing his Ph.D. degree in the Department of Civil Engineering at Kunsan National University, Republic of Korea. His research interests include coastal and hydraulic engineering, sediment transport and erosion/deposition analysis, sediment grain size analysis, physical oceanography, marine environmental monitoring, and overall data analysis and field surveys in the aquatic environment sector. (hgs712@hanmail.net)

**Seung-Bae Choi** is currently pursuing his Ph.D. degree at Kunsan National University, Republic of Korea. His research interests include coastal engineering, sediment transport, physical oceanography, environmental monitoring, and data analysis for coastal engineering. (ace8978@kunsan.ac.kr)

**Jae-Seon Yoon** received his Ph.D. degree in civil engineering from Hanyang University, majoring in water resources and coastal engineering. He is currently conducting various numerical and hydraulic model studies at the Rural Research Institute of the Korea Rural Community Corporation. (jsun0757@ekr.or.kr)

**Woochul Kang** received his Ph.D. degree from Colorado State University, USA, in 2019. From 2019 to 2024, he was a researcher at the Korea Institute of Civil Engineering and Building Technology (KICT). He is currently an assistant professor at Kongju National University. While his research interests cover a wide range of fields, his main area involves integrating water engineering—his primary major—with various technologies such as remote sensing and AI. (kang@kongju.ac.kr)

**Hyung-Suk Kim** received his Ph.D. degree in civil engineering from Hokkaido University, Japan in 2013. From 2013 to 2020, he served as a junior and senior researcher at the Korea Institute of Civil Engineering and Building Technology (KICT). Since 2020, he has been an assistant professor in the Department of Civil Engineering at Kunsan National University, Republic of Korea. His research interests include hydraulics and coastal engineering, sediment transport and riverbed dynamics, scouring, and ecological modeling of fish populations. (hskim0824@kunsan.ac.kr)